A Primer of Negative Test Dimensions and Degrees of Emptiness of Latent Sets

Benoit B. Mandelbrot[a,b] and Michael Frame[b*]
[a]Pacific Northwest National Laboratory and [b]Yale University

February 27, 2007

1 Introduction

Fractal geometry made useful in the sciences – commonplace even, and known to general audiences – the facts that dimension exhibits several distinct interpretations and that some sets have important properties best described by non-integer values of dimension. At first this is counterintuitive because in the analytic geometry of Descartes the term "(Euclidean) dimension" D_E is interpreted as the "number of independent directions." This common interpretation is important because it generalizes our experience with the physical world, but dimension has many other meanings. Fractal geometry uses dimension to give quantitative measures of the notion of roughness. These measures include the similarity dimension D_s (recalled in section 4), the box-counting dimenson D_b (recalled in section 5) of Minkowski and Bouligand, the Hausdorff dimension (see chapter 2 of [7]), and the packing dimension D_p (not used in this analysis, but useful in many contexts, see chapter 3 of [7]).

This paper presents a simple exposition and illustrative examples of the next step, from degrees of roughness to degress of emptiness, a direction first explored in [13], [15], [14], [16], [17], [18], and made rigorous in [3]. Degrees of roughness and emptiness can be quantified through the notion of *test dimension*, D_t, introduced in section 6. When it is positive, $D_t = D_b$; when it is negative and the set is almost surely empty, D_t measures the emptiness of a *latent set*, a concept introduced in section 7 and replacing the universal empty set with a multitude of cases referencing the process by which the set became empty. This may seem counterintuitive, but can be measured empirically and already has shown its usefulness, for example in engineering problems [4], [5] involving multifractals, and in clusters in statistical physics [6]. The table below is a summary of some of the principal types of dimension. One goal of this paper is to introduce the test dimension, D_t.

*Both authors were partially supported by NSF DMS 0203203

D_{top}	topological	connectivity
D_E	Euclidean	cardinality of a basis
D_s	similarity	scaling under decomposition
D_h	Hausdorff-Besicovitch	discontinuity of measure
D_b	box-counting	scaling of coverings
D_p	packing	scaling of packings
D_t	test	roughness/emptiness

Central to the concept of test dimension is the distinction that while dimension often is seen as referring to the set, in some cases dimension refers to the process generating the set. For instance, consider a self-similar set consisting of N copies of itself, each scaled by a factor r. The Sierpinski gasket, shown on the right side of Fig. 1, consists of $N = 3$ copies of itself, each scaled by $r = \frac{1}{2}$. The similarity dimension is given by the familiar formula $D_s = \log(N)/\log(1/r)$, $\log(3)/\log(2)$ for the gasket. As illustrated in the first three images of Fig. 1, these numbers describe the generating process: replace each copy of the triangle by $N = 3$ copies, each scaled by a factor of $r = \frac{1}{2}$.

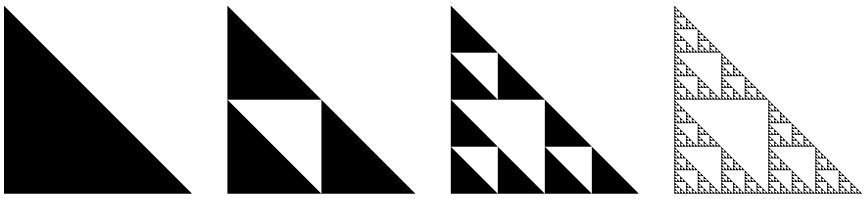

Figure 1: A process generating the Sierpinski gasket

In familiar cases such as the gasket, the description of the set and its construction appear to be equivalent; for some random fractals, the set and generating process generalize differently.

Indeed, suppose that at each stage of the construction this process involves a random N, so many samples of the limiting process create a population of fractals. In this case, the similarity dimension is redefined as $\log(E(N))/\log(1/r)$, where $E(N)$ denotes the expected value of N. If $E(N) > 1$, then for almost all sample limits this expression coincides with the values that other definitions (such as D_b and D_h) assign to the sample limit set.

This leads to the unconventional case when $E(N) < 1$, hence

$$\log(E(N))/\log(1/r) < 0.$$

The construction of the preceding paragraph almost surely produces an empty limit set. Classical dimension theory [10] allows only one negative dimension, for the empty set $D_{top} = -1$. The uniqueness of this value confirms that in common mathematical thinking, the empty set is unique: the set consisting of no oranges is identical to the set consisting of no apples.

To avoid possible confusion arising from studying "degrees of emptiness of the empty set," the name *latent set* is assigned to the almost surely empty

limit of iterative processes with $E(N) < 1$. Because this refers refer to samples of random processes, the dimension is called the "test dimension." "Sample dimension" was another possibility; the shorter term is preferrable. A goal of this paper is to show that different negative values of D_t distinguish between latent sets of different degrees of emptiness, that is, between almost impossible events of various degrees of almost impossibility.

The objects for which the negative test dimension first was developed were not fractal or Euclidean sets, but multifractal measures, revealed in the study of turbulence. Negative dimensions in the context of multifractal measures is taken up in the sequel [19].

It should be noted that a non-geometric negative dimension, unrelated to test dimension or to fractals, goes back at least to [11].

This extension of dimension into the negative range follows the pattern of folk history: that negative numbers replaced the unique notion of "being in debt" by multiple notions of "owning some negative amount of money." This requires embedding the positive axis in the real line. Imaginary numbers began as quantities needed to be able to solve all quadratic equations; the step that gave them a geometric interpretation consisted in embedding the real line in the plane. Similarly, embedding is a key step for interpreting negative test dimensions.

2 Some algebra of dimensions of Euclidean sets

The dimensions of ordinary Euclidean sets are non-negative integers which obey several rules that are rarely stated (though well-known) but are intuitively plausible, and, under additional conditions, are rigorously provable. For example,

monotonicity if $A \subseteq B$, then $\dim(A) \leq \dim(B)$,

union typically, the dimension of the union of two sets is the maximum of the dimensions of the sets: $\dim(A \cup B) = \max\{\dim(A), \dim(B)\}$,

product typically, the dimension of the Cartesian product of two sets is the sum of the dimensions of the sets: $\dim(A \times B) = \dim(A) + \dim(B)$,

and

intersection typically, the codimension of the intersection of two sets is the sum of the codimensions of the sets: $E - \dim(A \cap B) = (E - \dim(A)) + (E - \dim(B))$, where A and B are subsets of $\mathbf{R}^E$. The intersection rule also is called the *codimension addition rule*. More directly, the rule is

$$\dim(A \cap B) = \dim(A) + \dim(B) - E. \tag{1}$$

With dimension as it is usually understood, however, the intersection rule is subject to what will be called a *key caveat*, analogous to early restrictions that

allowed subtraction only if the difference was nonnegative, or square roots only if the radicand was nonnegative.
Key caveat: when the intersection rule yields $\dim(A \cap B) = \delta < 0$, then typically $A \cap B$ is empty.

Does it follow that these negative values of δ are an idle imaginary product of formal manipulation let loose? Or perhaps δ has no reality but can be assigned some redeeming practical value? The terms "imaginary" and "real" have been choosen to hint at things to come.

Mandelbrot [12] generalized these rules of algebra of dimensions to random fractals, and interpreted negative test dimensions as measures of a *degree of emptiness* (see section 7).

3 The codimension addition rule: examples and a first glimpse of negative-valued formal dimensions

To illustrate the codimension addition rule, the least-familiar of the four algebra of dimension rules, suppose A and B are planes in $\mathbf{R}^3$. Then

$$3 - \dim(A \cap B) = (3 - \dim(A)) + (3 - \dim(A)) = 2$$

and so $\dim(A \cap B) = 1$: planes in space typically intersect in a line.

If A is a plane and B is a line in $\mathbf{R}^3$, the analogous calculation yields $\dim(A \cap B) = 0$: in space a plane and a line typically intersect in a point. If A and B are lines in $\mathbf{R}^3$, then $\dim(A \cap B) = -1$: in space two lines typically do not intersect at all, that is, intersect in the empty set.

To construct more examples, note the intersection rule generalizes to intersections of more than two sets. For instance,

$$E - \dim(A \cap B \cap C) = (E - \dim(A)) + (E - \dim(B)) + (E - \dim(C))$$

where A, B and C are subsets of $\mathbf{R}^E$. For a Euclidean example, three planes in $\mathbf{R}^3$ typically intersect in a point. Fig. 2 shows some other examples. Here all pictures take place in $\mathbf{R}^3$. All but the first two have negative dimensions, increasingly negative proceeding through the figure. Very roughly, the more negative the dimension, the more easily the components miss one another.

For the notion of negative dimensions to become precise, randomness is injected and Minkowski's approach to dimension is modified by replacing his notion of ϵ-neighborhood by a notion of ϵ pseudo-neighborhood. First, in sections 4 and 5 the notions of similarity and box-counting dimensions are reviewed.

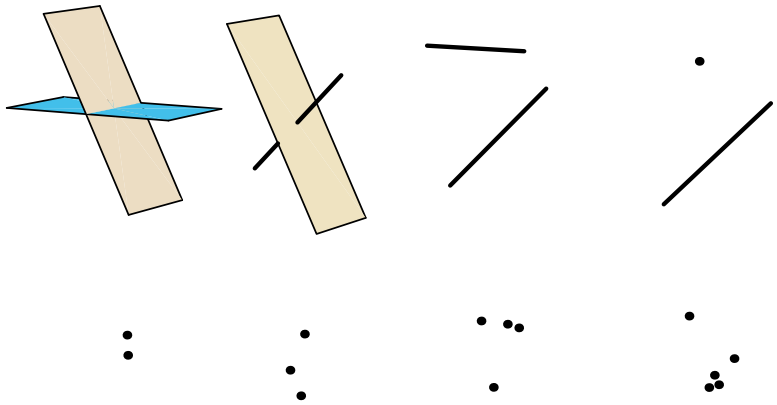

Figure 2: Left to right, top to bottom: the codimension addition rule gives typical intersections of dimension 1, 0, -1, -2, -3, -6, -9, and -12.

4 The (always positive) similarity dimension

For a self-simialr set consisting of N pieces, each linearly scaled by the same factor of r, the similarity dimension is

$$D_s = \frac{\log(N)}{\log(1/r)} \tag{2}$$

For example, the Sierpinski gasket (Fig. 3, left) consists of $N = 3$ pieces, each scaled by a factor of $r = \frac{1}{2}$, so as seen in 1 the similarity dimension of the gasket is $D_s = \log(3)/\log(2)$.

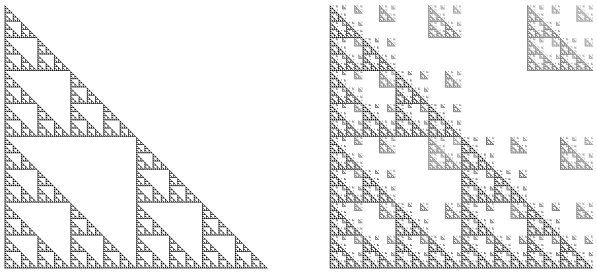

Figure 3: Left: the Sierpinski gasket, consisting of 3 pieces scaled by $\frac{1}{2}$. Right: a self-similar fractal consisting of 3 pieces scaled by $\frac{1}{2}$ and one piece scaled by $\frac{1}{4}$.

This notion is extended easily to self-similar sets for which different pieces are scaled by different factors. Suppose the set F can be written as $F = F_1 \cup \cdots \cup F_N$ with each F_i a copy of F scaled by a factor r_i. To accommodate these different values for r_i, note equation (2) can be rewritten as

$$1 = N \cdot r^{D_s} = r^{D_s} + \cdots + r^{D_s}$$

Replacing each r with an r_i gives rise to the *Moran equation*:

$$\sum_{i=1}^{N} r_i^D = 1 \tag{3}$$

If each r_i satisfies $0 < r_i < 1$, analyzing the graph of $f(r) = \sum_i r_i^D$ shows the Moran equation has a unique solution, $D = D_s$. The right side of Fig. 3 shows a self-similar set consisting of 3 pieces scaled by $\frac{1}{2}$ and one piece scaled by $\frac{1}{4}$. The Moran equation $3(\frac{1}{2})^D + (\frac{1}{4})^D = 1$ can be rewritten as the quadratc equation $x^2 + 3x - 1 = 0$ in $x = (\frac{1}{2})^D$. Solving gives $D = \log((-3 + \sqrt{13})/2)/\log(1/2)$.

Under fairly general conditions (for example, Hutchinson's Open Set condition [9] and section 9.2 of [7]), the similarity dimension equals the Hausdorff dimension D_H, a quantity of great importance but often difficult to compute.

5 The (always-positive) box-dimension of Minkowski-Bouligand

The similarity dimension is computed easily, but is defined only for self-similar sets. Among the dimensions defined for more general sets, the box-counting dimension is computed most easily. We follow Minkowski's approach. For any subset $A \subset \mathbf{R}^E$, denote by A_ϵ the ϵ-neighborhood (nbhd) of A:

$$A_\epsilon = \{x \in \mathbf{R}^E : dist(x, z) \leq \epsilon \text{ for some } z \in A\}$$

Minkowski argued that for a d-dimensional Euclidean set $A \subset \mathbf{R}^E$, $\mathrm{vol}(A_\epsilon)$ scales as ϵ^{E-d}, and Bouligand extended this to the case on non-integer d, but for which dimension d? The correct dimension is the box-counting dimension D_b.

Assuming $vol(A_\epsilon) \sim k\epsilon^{E-d}$ for some constant k, and assuming the approximation gets better for smaller ϵ,

$$D_b(A) = E - \lim_{\epsilon \to 0} \frac{\log(vol(A_\epsilon))}{\log(\epsilon)} \tag{4}$$

with the understanding that if the limit does not exist, it is replaced with $\overline{\lim}$ and $\underline{\lim}$, obtaining lower and upper box-counting dimensions $\underline{D}_b(A)$ and $\overline{D}_b(A)$. See Prop. 3.2 of [7] for an accessible development.

Example 5.1 *Computing the dimension of the Sierpinski gasket by the Minkowski-Bouligand approach.*

Suppose the altitude and base of the gasket G have length 1. Denote by ϵ_1 the smallest value of ϵ for which G_ϵ has no holes, by ϵ_2 the smallest value of ϵ for which G_ϵ has a single hole, by ϵ_3 the smallest value of ϵ for which G_ϵ has four holes, and so on. Some straightforward geometry gives

$$\epsilon_n = \frac{1}{2^n(2+\sqrt{2})}$$

To understand the pattern of G_{ϵ_n}, observe that G_{ϵ_1} is the filled-in triangle, together with a band of width ϵ_1, so

$$Area(G_{\epsilon_1}) = \frac{1}{2} + (2+\sqrt{2})\epsilon_1 + \pi\epsilon_1^2 = \frac{1}{2} + P(\epsilon_1)$$

where $P(\epsilon_1)$ denotes the area of the part of the ϵ_1-nbhd of the gasket perimeter lying outside the perimeter. On the left of Fig. 4 is the gasket; center and right are ϵ-nbhds G_ϵ for $\epsilon_1 > \epsilon > \epsilon_2$ and $\epsilon_2 > \epsilon > \epsilon_3$. Note as $\epsilon \to 0$, in G_ϵ more and more holes arise and existing holes become enlarged.

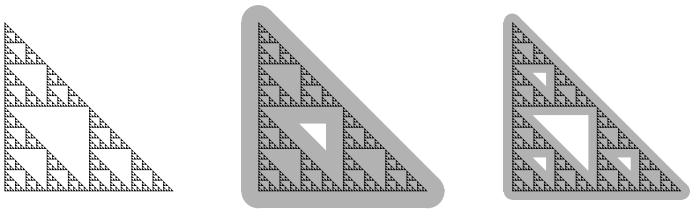

Figure 4: The gasket and two ϵ-nbhds.

Next, G_{ϵ_2} is the filled-in triangle with a hole having vertices $(\frac{1}{2},0),(\frac{1}{2},\frac{1}{2})$ and $(0,\frac{1}{2})$, together with a band of width ϵ_2 along the outside and inside edges, leaving a triangular hole with base and altitude $\frac{1}{2} - (1+\sqrt{2})\epsilon_2$. Thus

$$Area(G_{\epsilon_2}) = \frac{1}{2} + P(\epsilon_2) - \frac{1}{2}\left(\frac{1}{2} - (1+\sqrt{2})\epsilon_2\right)^2$$

With each successive ϵ_n, more triangular holes open, yielding

$$Area(G_{\epsilon_n}) = \frac{1}{2} + P(\epsilon_n) - \frac{1}{2}\left(\frac{1}{2} - (1+\sqrt{2})\epsilon_n\right)^2 - \cdots - \frac{1}{2}3^{n-2}\left(\frac{1}{2^{n-1}} - (1+\sqrt{2})\epsilon_n\right)^2$$

Expanding the squared terms, grouping like powers of ϵ_n, summing the finite geometric series, and simplifying, yields

$$Area(G_{\epsilon_n}) = P(\epsilon_n) + \frac{1}{2}\left(\frac{3}{4}\right)^{n-1} - (1+\sqrt{2})\epsilon_n\left(1 - \left(\frac{3}{2}\right)^{n-1}\right) + \frac{1}{4}((1+\sqrt{2})\epsilon_n)^2(1-3^{n-1})$$

$$= \epsilon_n + \left(\pi + \frac{3+2\sqrt{2}}{4}\right)\epsilon_n^2 + \frac{1}{2}\left(\frac{3}{4}\right)^{n-1} + (1+\sqrt{2})\epsilon_n\left(\frac{3}{2}\right)^{n-1} - \frac{1}{4}(1+\sqrt{2})\epsilon_n^2 3^{n-1}$$

Noting $\left(\frac{3}{2^k}\right)^{n-1} = \frac{2^k}{3}(2+\sqrt{2})^{k-\log(3)/\log(2)}\epsilon_n^{k-\log(3)/\log(2)}$ for $k = 0, 1, 2$, gives

$$Area(G_{\epsilon_n}) = \epsilon_n + \left(\pi + \frac{3+2\sqrt{2}}{4}\right)\epsilon_n^2 + K\epsilon_n^{2-\log 3/\log 2}$$

where K is a constant, equal to $\frac{79+55\sqrt{2}}{12}(2+\sqrt{2})^{-\log 3/\log 2}$. The scaling behavior of $Area(G_{\epsilon_n})$ as $\epsilon_n \to 0$ is dominated by the smallest power of ϵ_n, which is $2 - \log 3/\log 2$. This can be seen by factoring out this power, to obtain

$$Area(G_{\epsilon_n}) = \left(\epsilon_n^{(\log 3/\log 2)-1} + \left(\pi + \frac{3+2\sqrt{2}}{4}\right)\epsilon_n^{\log 3/\log 2} + K\right)\epsilon_n^{2-\log 3/\log 2}$$

As $\epsilon_n \to 0$, the coefficient of $\epsilon_n^{2-\log(3)/\log(2)}$ goes to K. That is, $Area(G_{\epsilon_n})$ scales as $\epsilon_n^{2-\log(3)/\log(2)} = \epsilon_n^{2-d}$, where d is the similarity dimension of the gasket G. □

An alternative approach applies less generally, but can be considerably simpler. Some fractals are embedded in each of a nested sequence of closed sets, *prefractals*, that are stages in a recursive construction of the fractal. Fig. 5 illustrates a sequence of five (gray) prefractals, stages in a recursive construction of the gasket.

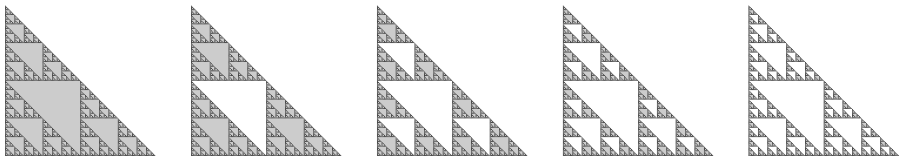

Figure 5: A sequence of prefractals approximating the gasket.

An area scaling relationship holds, with the continuous family of ϵ-nbhds replaced by the family of prefractals. For example, denoting by G_k the k^{th} prefractal of the gasket, so Fig. 5 shows G_0, G_1, G_2, G_3, the scaling hypothesis becomes

$$Area(G_k) \sim (2^{-k})^{2-d} \tag{5}$$

where 2^{-k} is the side length of the smallest filled-in triangle of G_k, the natural length scale of G_k. An easy calcualtion gives $Area(G_k) = \frac{1}{2}(\frac{3}{4})^k$. Combining this with equation (5) yields $\frac{1}{2}(\frac{3}{4})^k = b(2^{-k})^{2-d}$. In the $k \to \infty$ limit this gives $d = \log(3)/\log(2)$.

6 Randomness and the (positive or negative) test dimension; the concept of pseudo-neighborhood

To begin with a simple illustration, consider the typical intersection of a line A and a point B in the plane. Neglecting the key caveat in the codimension

addition rule gives

$$2 - \dim(A \cap B) = (2 - \dim(A)) + (2 - \dim(B)) = 3$$

This suggests $\dim(A \cap B) = -1$. The absurdity of this result is what motivates the key caveat. How can $\dim(A \cap B) = -1$ be made sensible?

To evaluate the box dimension by the Minkowski-Bouligand approach, calculate how $Area((A \cap B)_\epsilon)$ scales with ϵ. This cannot be done because typically $A \cap B$ is empty.

One approach to this problem involves two steps. First, replace $(A \cap B)_\epsilon$ with $A_\epsilon \cap B_\epsilon$, called an *$\epsilon$-pseudonbhd*, and test how its measure scales with ϵ. If $A \cap B \neq \emptyset$, the ϵ-nbhd $(A \cap B)_\epsilon$ and the ϵ-pseudonbhd $A_\epsilon \cap B_\epsilon$ exhibit the same scaling relation. This is illustrated in Example 6.1.

Example 6.1 *Comparing the ϵ-scalings of $(A \cap B)_\epsilon$ and of $A_\epsilon \cap B_\epsilon$.*

Let A and B be the rectangles $A = \{(x, y, 0) : 0 \leq x \leq 1, -1 \leq y \leq 1\}$ and $B = \{(x, 0, z) : 0 \leq x \leq 1, -1 \leq z \leq 1\}$. Then $A \cap B = \{(x, 0, 0) : 0 \leq x \leq 1\}$ and $(A \cap B)_\epsilon$ consists of a cylinder with radius ϵ and axis L, together with two hemispherical caps. Its volume is

$$Volume((A \cap B)_\epsilon) = \pi L \epsilon^2 + \frac{4}{3}\pi\epsilon^3 = (\pi L + \frac{4}{3}\pi\epsilon)\epsilon^2 \tag{6}$$

The ϵ-pseudonbhd $A_\epsilon \cap B_\epsilon$ is a parallelopiped with cross-section a square of side length 2ϵ and width L, together with two endcaps, the intersections of the cylinders of radius ϵ along the edges of the rectangles. Its volume is

$$Volume(A_\epsilon \cap B_\epsilon) = (2\epsilon)^2 L + 2\frac{8}{3}\epsilon^3 = (4L + \frac{16}{3}\epsilon)\epsilon^2 \tag{7}$$

Comparing equations (6) and (7) reveals that the volumes of both $(A \cap B)_\epsilon$ and $A_\epsilon \cap B_\epsilon$ scale as $\epsilon^2 = \epsilon^{3-1}$. That is, the scaling of the ϵ-pseudonbhd detects the dimension of $A \cap B$ in the same way as that of the ϵ-nbhd. □

This first step is not sufficient to extend the analysis to empty $A \cap B$: for disjoint compact sets A and B, $A_\epsilon \cap B_\epsilon$ is empty for small enough ϵ. To overcome this problem, the second step consists of sampling at randomly placed points P, computing the expected number $E(N(\epsilon))$ of points P for which P_ϵ intersects both A and B, and calculating how $E(N(\epsilon))$ scales with ϵ. Because this scaling relation is investigated for $\epsilon > 0$, this is called the *pre-asymptotic range*. This calculation is performed for many different placements of A and B, and the results averaged.

That is, the object of study is not the set, which after all is almost surely empty, but rather a process yielding the set. This is precisely in the spirit of the similarity dimension which is defined directly from a process, rather than just as the product of that process.

Example 6.2 *Scaling of the ϵ-pseudonbhd of a line and a point in the plane.*

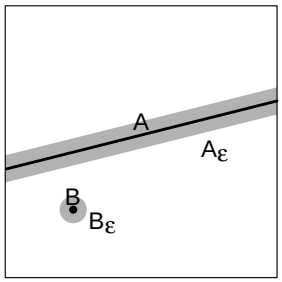

Figure 6: A line A and a point B in a box of side length L, together with their ϵ-nbhds A_ϵ and B_ϵ

Consider a line A and a point B both lying in a square S of side length L. Then A_ϵ intersects B_ϵ if $B \in A_{2\epsilon}$. Within S, $A_{2\epsilon}$ occupies an area of $k \cdot L \cdot 4\epsilon$, where k is a factor depending on the slope and placement of A. For horizontal and vertical lines, $k = 1$; for the lines passing through opposite corners of the box, k is slightly less than $\sqrt{2}$. ("Slightly less" because the corners of $A_{2\epsilon}$ lie outside S.) Given A and B placed uniformly randomly within S, the probability that $B \in A_{2\epsilon}$ is $Area(A_{2\epsilon})/(Area(S)) = (k \cdot L \cdot 4\epsilon)/L^2$, and so

$$Pr\{A_\epsilon \cap B_\epsilon \neq \emptyset\} = \frac{k \cdot 4\epsilon}{L}$$

Because B is a point, $N(\epsilon)$, the minimum number of squares of side length ϵ needed to cover $A_\epsilon \cap B_\epsilon$, is at most 1. Note

$$N(\epsilon) = \begin{cases} 1, & \text{if } A_\epsilon \cap B_\epsilon \neq \emptyset \\ 0, & \text{if } A_\epsilon \cap B_\epsilon = \emptyset \end{cases} \tag{8}$$

Thus

$$E(N(\epsilon)) = 0 \cdot Pr\{N(\epsilon) = 0\} + 1 \cdot Pr\{N(\epsilon) = 1\} = \frac{4k}{L}\epsilon \tag{9}$$

and consequently the test dimension $D_t(A \cap B)$ can be computed plausibly as

$$D_t(A \cap B) = \lim_{\epsilon \to 0} \frac{\log(E(N(\epsilon)))}{\log(1/\epsilon)} = -1. \tag{10}$$

Alternately, following Minkowski,

$$E(Area(A_\epsilon \cap B_\epsilon)) \sim \epsilon^{2-d}. \tag{11}$$

Estimating $E(Area(A_\epsilon \cap B_\epsilon))$ by $E(N(\epsilon))\epsilon^2$ and using equation (9) shows the area scales as ϵ^3. The result $d = -1$ is recovered by comparing this with equation (11). □

Example 6.3 *Scaling of the ϵ-pseudonbhd of a line and a point in space.*

If A and B are a line and a point in $\mathbf{R}^3$, then except near the edges of the cube, A_ϵ is a cylinder of radius ϵ. Consequently,

$$Pr\{A_\epsilon \cap B_\epsilon \neq \emptyset\} = \frac{k \cdot 4\epsilon^2 L}{L^3}$$

and as before the average box-counting dimension of $A \cap B$ can be computed plausibly as

$$\lim_{\epsilon \to 0} \frac{\log(E(N(\epsilon)))}{\log(1/\epsilon)} = -2.$$

Or again, following Minkowski, $E(Volume(A_\epsilon \cap B_\epsilon)) \sim \epsilon^{3-d}$ and estimating the average volume by $E(N(\epsilon))\epsilon^3$, recovering $d = -2$.

This reinforces our intuition that a point has more opportunity to miss a line in $\mathbf{R}^3$ than in $\mathbf{R}^2$. □

To help clarify the interpretation, note that here $E(N)$ refers not to a single construction, but to an average over a random ensemble of instances.

7 The example of birth and death fractals, manifest or latent

In section 5, a sequence of ϵ nbhds was viewed as a process. This is something of a stretch; in many cases, a set indeed is defined as the limit of a sequence of embedded nbhds, but often these are not ϵ-nbhds of the limit. However, the previous approach readily extends to random fractal sets, defined as limits of prefractals (a non-random variant is described at the end of section 5), each of which is a collection of $N(\epsilon)$ cubes of side length ϵ. Generalizing equation (10), define the test dimension D_t by

$$D_t = \lim_{\epsilon \to 0} \frac{\log(E(N(\epsilon)))}{\log(1/\epsilon)} \tag{12}$$

When the limit exists and is negative, as in the Euclidean examples of section 5, it reduces to an approach based on pseudonbhds and both defines and measures the degree of emptiness.

Birth and death processes provide good examples. See [1] and [8] for general references, and chapter 23 of [12] for an application to random fractals. Example 7.1 illustrates the basic concepts of these processes.

Example 7.1 *Birth and death in the unit square.*

Start with the unit square S. Subdivide S into four congruent subsquares, S_0, S_1, S_2, and S_3, and assign the probabilities p_0, p_1, p_2, and p_3, with $\sum_i p_i = 1$, of *surviving* from S to S_i. Subdivide each surviving S_i into four congruent subsquares S_{i0}, S_{i1}, S_{i2}, and S_{i3}, and assign each the corresponding probability $p_{ij} = p_j$ for $j = 0, 1, 2, 3$. Continue. Subsquares of side length 2^{-k} have *length* k

addresses denoted by the subscript of $S_{i_1 \ldots i_k}$. Using the familiar IFS formalism [2] with transformations

$$T_i(x, y) = \left(\frac{x}{2}, \frac{y}{2}\right) + (a_i, b_i)$$

where $(a_i, b_i) = (0,0), \left(\frac{1}{2}, 0\right), \left(0, \frac{1}{2}\right), \left(\frac{1}{2}, \frac{1}{2}\right)$ for $i = 0, 1, 2, 3$, it follows that

$$S_{i_1 i_2 \ldots i_k} = T_{i_1}(T_{i_2}(\cdots T_{i_k}(S)\cdots))$$

Note the inclusions

$$S_{i_1} \supset S_{i_1 i_2} \supset \cdots \supset S_{i_1 i_2 \ldots i_k}$$

Associated with each subsquare is a sequence $\{p_{i_1}, p_{i_1 i_2}, \ldots, p_{i_1 i_2 \ldots i_k}\}$ of probabilities. Now a picture of a canonical fractal dust can be generated by selecting a threshold survival probability p_s and filling the square if

$$\max\{p_{i_1}, p_{i_1 i_2}, \ldots, p_{i_1 i_2 \ldots i_k}\} < p_s$$

Otherwise, leave the subsquare empty. Fig. 7 shows some examples, with p_s decreasing from left to right.

At each level, p_s is the probability that a particular subsquare is occupied. The number, N, of occupied subsquares satisfies

$$\begin{aligned}
N = 0 &\quad \text{with probability } (1-p_s)^4 \\
N = 1 &\quad \text{with probability } 4(1-p_s)^3 p_s \\
N = 2 &\quad \text{with probability } 6(1-p_s)^2 p_s^2 \\
N = 3 &\quad \text{with probability } 4(1-p_s) p_s^3 \\
N = 4 &\quad \text{with probability } p_s^4
\end{aligned}$$

Then the expected number of occupied subsquares of a square is

$$0 \cdot (1-p_s)^4 + 1 \cdot 4(1-p_s)^3 p_s + 2 \cdot 6(1-p_s)^2 p_s^2 + 3 \cdot 4(1-p_s) p_s^3 + 4 \cdot p_s^4 = 4p_s$$

and the expected number of occupied subsquares of side length 2^{-k} is $E(N(2^{-k})) = (4p_s)^k$. The test dimension is

$$D_t = \lim_{k \to \infty} \frac{\log(E(N(2^{-k})))}{\log(2^k)} = 2 + \log_2(p_s) \tag{13}$$

Fig. 7 shows instances for which $D_t = 1.6, 1.3, 1.0$, and 0.7. Anticipating the next section, through each square take an arbitrary horizontal cut. This is the result of the same construction applied to an interval successively divided in half, with the dimension D_t reduced by 1. When $D_t > 1$ the cross-section has a positive probability of being non-empty. As the second square of Fig. 7 shows, positive probability does not guarantee every instance is non-empty. □

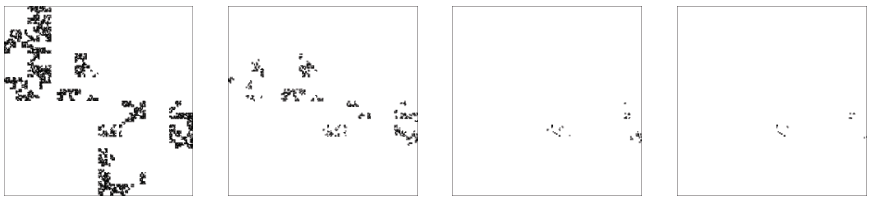

Figure 7: A sequence of birth and death canonical fractal sets. From left to right the dimensions are $1.6, 1.3, 1.0$, and 0.7.

To express this in the standard language of branching processes, observe that each occupied square can have $i = 0$ to 4 occupied subsquares. Denote by $\hat{p}_i$ the probability of having i occupied subsquares. These were computed above, for example, $\hat{p}_1 = 4(1-p_s)^3 p_s$. Denote by Z_n the number of occupied squares in the n^{th} generation. The extinction theorem proved by Steffensen (page 7 of [8]) shows the probability that nothing survives to the limit is 1 if $f'(1) = E(Z_1) \leq 1$, where $f(s) = \sum_{n=0}^{4} \hat{p}_n s^n$ is the probability generating function. As calculated above, $f'(1) = 4p_s$. When $f'(1) > 1$, the probability that nothing survives to the limit is the unique solution $s = \xi(p_s)$ of $s = f(s) = ((1-p_s) + p_s s)^4$ in the interval $(0, 1)$. This solution is

$$\xi(p_s) = 1 - \frac{4}{3p_s} - \frac{2^{4/3}p_s^2}{3\rho(p_s)} + \frac{\rho(p_s)}{3 \cdot 2^{1/3} p_s^4} \tag{14}$$

where $\rho(p) = ((27 + 3\sqrt{3}\sqrt{27 - 40p + 16p^2})p^8 - 20p^9)^{1/3}$. Note $\xi(\frac{1}{4}) = 1$ and as $p_s \to 0$, $\xi(p_s)$ decreases rapidly to 0.

In the construction illustrated by Fig. 7, this suggests two cases: *manifest*, with $D_t > 0$, and *latent*, with $D_t < 0$. In the latent case, almost surely the set is empty and D_t quantifies the process by which the set arrives at being empty. The manifest case has two subcases, corresponding to the limit's being empty and non-empty.

The manifest case $p_s > \frac{1}{4}$. In this case, equation (13) implies $D_t > 0$. Given that $E(N) > 1$, well-known resultss from the theory of birth and death processes (see pgs 12 - 14 of [8]) can be applied and show that after k stages the number of occupied subsquares takes the form $\Phi E(N)$, where the prefactor Φ is a random variable that goes to 0 only when nothing survives in the limit. This random prefactor is a consequence of large fluctuations that can occur in early generations. Then a refinement of equation (13) is

$$D_t = 2 + \log_2(p_s) + \frac{\log(\Phi)}{\log(2^k)}.$$

As $k \to \infty$, this converges to the value $2 + \log_2(p_s)$ obtained by the simpler calculation.

Note that an empty limit can result even when $E(N) > 1$. Through the process of supersampling, described in section 9, a positive dimension can be associated even with this situation.

The latent case $p_s < \frac{1}{4}$. In this case, $D < 0$. Given that $E(N) < 1$, from Steffensen's extinction theorem it follows that the limit is almost surely empty. This conclusion used to be the end of the story, but sections 8 and 9 show ways in which this analysis can be continued.

8 Life beyond death I: the process of linear intersection and embedding; critical embedding dimension

Carrying out the construction of Example 7.1 applied to subdividing E-dimensional cubes yields random birth and death fractals with

$$D_t = E + \log_2(p_s)$$

Consequently, for a given threshold probability p_s there is a critical embedding dimension

$$E_{crit} = [\![-\log_2(p_s)]\!] \tag{15}$$

where $[\![x]\!]$ is the smallest integer $\geq x$, so that for all test dimensions $E > E_{crit}$ the birth and death set has a positive probability of being non-empty and of positive dimension. Then for every p_s, *birth and death fractals with negative test dimension are the intersections between positive test dimension birth and death fractals constructed in* $\mathbf{R}^E$*, with* $E > E_{crit}$*, and appropriate linear subspaces of* $\mathbf{R}^E$.

Example 8.1 *Birth and death in the Sierpinski gasket.*

Start with the unit square S, subdivide it into four congruent subsquares, S_0, S_1, S_2, and S_3, and delete S_3, the upper right square. Assign probabilities p_0, p_1, and p_2 to subsquares S_0, S_1, and S_2. Subdivide each S_i into four congruent subsquares and delete the upper right subsquare, obtaining S_{i0}, S_{i1}, and S_{i2}. Assign each a probability p_{i0}, p_{i1}, and p_{i2}. Continue. Write $\mathbf{S}_1 = S_0 \cup S_1 \cup S_2$, $\mathbf{S}_2 = S_{00} \cup S_{01} \cup S_{02} \cup S_{10} \cup \cdots \cup S_{22}$, and so on. In the classical language of convergence in the Hausdorff metric ([9], chapter 9 of [7]), the $\mathbf{S}_i$ converge to the right isosceles Sierpinski gasket G generated by the IFS transformations T_0, T_1, and T_2 or example 7.1. Selecting a threshold probability p_s and preceding as in example 7.1, the expected number of occupied subsquares of a square is

$$0 \cdot (1-p_s)^3 + 1 \cdot 2(1-p_s)^2 p_s + 3 \cdot 2(1-p_s)p_s^2 + 3 \cdot p_s^3 = 3p_s$$

and the expected number of occupied subsquares of side length 2^{-k} is $E(N(2^{-k})) = (3p_s)^k$. Call the limit set $G(p_s)$. The test dimension of $G(p_s)$ is

$$D_t = \frac{\log((3p_s)^k)}{\log(2^k)} = \frac{\log(3)}{\log(2)} + \frac{\log(p_s)}{\log(2)}$$

Note of course $D_t \leq \log(3)/\log(2)$ and $D_t \to \log(3)/\log(2)$ as $p_s \to 1$.

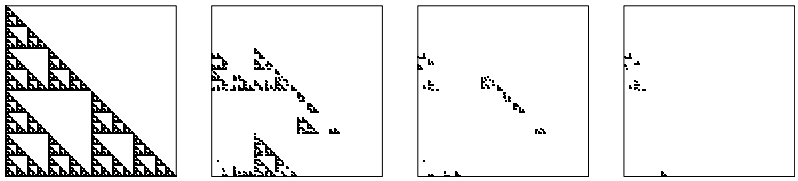

Figure 8: A sequence of birth and death canonical fractal sets.

If L is an arbitrary line crossing the square, then the intersection formula gives

$$D_t(G(p_s) \cap L) = D_t(G(p_s)) - 1$$

So as long as $D_t(G(p_s)) > 1$, there is a positive probability that a linear cut through $G(p_s)$ is non-empty and has positive dimension. See Fig. 8. From left to right the test dimensions are $\log(3)/\log(2), \log(3)/\log(2) - 0.2 \approx 1.38496, \log(3)/\log(2) - 0.4 \approx 1.18496$, and $\log(3)/\log(2) - 0.6 \approx 0.98469$. □

Examples 7.1 and 8.1 have been special in that the IFS are similarities with the same contraction factor. Example 8.2 shows this approach can be applied in a more general setting.

Example 8.2 *Birth and death in a fractal with different scaling factors.*

Consider the IFS with transformations T_0, T_1, and T_2 of Example 7.1, together with $T_3(x, y) = (x/4, y/4) + (3/4, 3/4)$. Call A the fractal generated by this IFS. The contraction factors are $r_0 = r_1 = r_2 = 1/2$ and $r_3 = 1/4$, so by the Moran equation (3) A has dimension $D = \log((3 + \sqrt{13})/2)/\log(2)$. See the left image of Fig. 9.

For a given p_s finding the number of occupied squares is more subtle than in the previous examples. Simply finding the number of squares for box-counting requires some thought. Inspecting the left image of Fig. 9 gives

$$N(2^{-1}) = 4 \qquad N(2^{-2}) = 13$$

Noting $T_0(A), T_1(A)$, and $T_2(A)$, the lower left, lower right, and upper left parts of A, are copies of A scaled by $\frac{1}{2}$, and $T_3(A)$, the upper right part of A, is a copy scaled by $\frac{1}{4}$, gives this relation for the number of boxes:

$$N(2^{-(n+1)}) = 3N(2^{-n}) + N(2^{-(n-1)})$$

To solve this difference equation, suppose $N(2^{-n}) = \lambda^n$. The difference equation becomes $\lambda^{n-1}(\lambda^2 - 3\lambda - 1) = 0$, with solutions $\lambda = (3 \pm \sqrt{13})/2$. Then the general form of $N(2^{-n})$ is

$$N(2^{-n}) = A\left(\frac{3 + \sqrt{13}}{2}\right)^n + B\left(\frac{3 - \sqrt{13}}{2}\right)^n$$

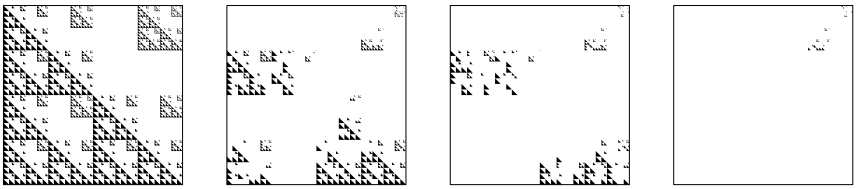

Figure 9: Another sequence of birth and death canonical fractal sets.

Using the initial conditions $N(2^{-1}) = 4$ and $N(2^{-2}) = 13$ to solve for A and B gives

$$N(2^{-n}) = \frac{2(26+7\sqrt{13})}{13(3+\sqrt{13})}\left(\frac{3+\sqrt{13}}{2}\right)^n + \frac{13-5\sqrt{13}}{26}\left(\frac{3-\sqrt{13}}{2}\right)^n$$

To compute the expected number of occupied subsquares of side length 2^{-n}, use

Lemma 8.1 $\displaystyle\sum_{k=0}^{n} k\binom{n}{k}p^k(1-p)^{n-k} = np$

The proof is a straightforward, if slightly tedious, inductive argument using

$$\binom{n}{k} = \binom{n-1}{k} + \binom{n-1}{k-1}$$

In examples 7.1 and 8.1, $N(2^{-(n+1)})$ is expressed as a function of $N(2^{-n})$ and so found a relation between the number of occupied subsquares in one generation and those in the next, thus finding $E(N(2^{-n}))$. Here the generational dependence of $N(2^{-n})$ is more complicated, but it is expressed as a formula of n alone. Recalling the random multiplier is applied in each generation, with Lemma 8.1,

$$E(N(2^{-n})) = \left(\frac{2(26+7\sqrt{13})}{13(3+\sqrt{13})}\left(\frac{3+\sqrt{13}}{2}\right)^n + \frac{13-5\sqrt{13}}{26}\left(\frac{3-\sqrt{13}}{2}\right)^n\right)p_s^n$$

The test dimension is

$$D_t = \lim_{n\to\infty}\frac{\log(E(N(2^{-n})))}{\log(2^n)} = \frac{\log((3+\sqrt{13})/2)}{\log(2)} + \frac{\log(p_s)}{\log(2)}$$

Note as $p_s \to 1$, D approaches the value obtained by the Moran equation (3). Fig. 9 shows examples of the associated birth and death fractal for several values of p_s. From left to right the dimensions are $D = \log((3+\sqrt{13})/2)/\log(2) \approx 1.72368, D - 0.25 \approx 1.47368, D - 0.5 \approx 1.22368$, and $D - 0.75 \approx 0.97368$. Note when $p_s < 1$ typically (with probability 1) a linear cross-section is empty. □

9 Life beyond death II: the process of supersampling

An alternative to embedding is the notion of supersampling, introduced in [13]. As an illustration, continue with the construction of Example 8.1. To this end, fix $\epsilon = 2^{-k}$ and recall $E(N(2^{-k})) = (4p_s)^k$. Denote by A the set generated by this birth and death process, and by L the line subtending the linear cross-section. Then

$$E(Area(A_\epsilon)) \leq E(N(\epsilon))\epsilon^2 = p_s^k$$

and

$$Area(L_\epsilon) \approx 2\epsilon = 2^{-k+1}$$

Recall the construction takes place within the unit square. Then

$$Pr\{A_\epsilon \cap L_\epsilon = \emptyset\} \leq \frac{Area(L_\epsilon)}{1 - Area(A_\epsilon)} \leq \frac{2^{-k+1}}{1 - p_s^k}$$

For sufficiently large k (larger for p_s closer to 1), this ratio is less than 1. That is, the probability that L_ϵ misses A_ϵ can be written as $1 - \eta$, for some $\eta > 0$.

Supersampling is the process of generating M such samples. The probability that are least one is nonempty is $1 - (1 - \eta)^M$, and arbitrarily close to 1. Now observe that η depends on p_s, which in turn depends on D_t through equation (13). Specifically,

$$M \geq \frac{\log(\delta)}{\log\big(2^{-k+1}/\big(1 - 2^{k(D_t-2)}\big)\big)}$$

where $(1-\eta)^M = \delta \ll 1$.Therefore, D_t quantifies the effort necessary to establish that an object that was counted as empty was, in fact, latent in the sense that it can change to manifest under supersampling.

Finally, note that in the case $p_s > \frac{1}{4}$, the limit still may be empty, with probability $\xi(p_s)$ given by equation (14). Then the probability that at least one of M such samples is nonempty is $1 - \xi(p_s)^M$. Writing $\xi(p_s) = \delta \ll 1$ gives

$$M = \frac{\log(\delta)}{\log(\xi(p_s))}$$

Comparing these two expressions for M illuminates the difference between latent and manifest. In the manifest case, the limit may be empty by bad luck; in the latent case, the limit may be nonempty by very, very good luck. The test dimension can be viewed as a quantificaiton of this luck.

10 Conclusion

The notion of negative dimension first imposed itself in the context of random multifractal measures. It is indispensable there, both in theory and practice, because it helps to unscramble a variety of forbiddingly complex possibilities.

However, sets are far simpler than measures and we found the task of introducing negative dimension to be most manageable in the context of problems concerning sets. We elected to start with the theorem that in three-dimensional space two lines intersect with zero probability. But any standard theorem that describes a more interesting property as having zero probability could also be extended automatically into a broad field that has hardly been explored. By allowing finer distinctions to be made, negative dimensions open up an infinity of potentially interesting questions.

To give an example, of ideas developed in [19], where more detail is provided, we may flash forward to random multifractal measures, which are defined as obeying certain scaling properties. Their most important characteristic is a certain function denoted by $f(\alpha)$. For the conventional nonrandom measures f is positive and quantifies certain fractal dimensional properties. But for random measures f, can take negative values as well. In very broad outline, the positive values characterize dimensional properties that are common to all, or almost all, individual sample measures, considered singly. The negative values serve a very different purpose: to help characterize the population of measures.

In the example of random measures on the interval [0,1], a key characteristic is the probability distribution of the measure Ω in the whole interval. When this distribution is long-tailed, there is a finite critical exponent q_{crit} such that $E(d\mu)^q$ diverges for $q > q_{crit}$ and converges for $q < q_{crit}$. A key theorem states that this exponent turns out to depend on $f(\alpha)s$ below 0, that is, on sets of negative dimension. Those sets would be grossly underestimated by being simply called empty. Since they manifest themselves by the values of traditional quantities that are directly observable, they can be called latent. We have seen that latent sets also can be made manifest by either of two procedures whose validity is broader than the finiteness of q_{crit}, namely, embedding as sections of higher-dimensional non-empty sets, and repeated sampling (supersampling) of a finite resolution constructions. Both approaches were suggested by and tested in experimental work in turbulence [4], [5].

Acknowledgement Comments by Rogene Eichler-West were helpful in the preparation of this manuscript.

References

[1] K. Atreya, P. Ney, *Branching Processes,* Springer, 1972.

[2] M. Barnsley, *Fractals Everywhere,* Academic Press, 1988.

[3] D. Beliaev, *Harmonic measures on random fractals,* Ph. D. thesis, Royall Institute of Technology, Stockholm, 2005.

[4] A. Chhabra, K. Sreenivasan, *Negative dimensions: theory, computation, and experiment,* Phys. Rev. A **43** (1991), 1114–1117.

[5] A. Chhabra, K. Sreenivasan, *Scale-invariant multiplier distributions in turbulence,* Phys. Rev. Lett. **68** (1992), 2762–2765.

[6] B. Duplantier, *Conformal fractal geometry and boundary quantum gravity,* in Fractal Geometry and Applications: A Jubilee of Benoit Mandelbrot Vol. 2, M. Lapidus and M. van Frankenhuijsen, eds., American Mathematical Society, 2004, 365–482.

[7] K. Falconer, *Techniques in Fractal Geometry*, Wiley, 1997.

[8] T. Harris, *The Theory of Branching Processes*, Springer-Verlag, 1963.

[9] J. Hutchinson, *Fractals and self-similarity,* Indiana Univ. Math. J. **30** (1981), 713–747.

[10] W. Hurewicz, H. Wallman, *Dimension Theory*, Princeton University Press. 1941.

[11] J. Lehner, *On modular forms of negative dimension,* Michigan Math. J. **6** (1959), 71–88.

[12] B. Mandelbrot, *The Fractal Geometry of Nature*, Freeman, 1982.

[13] B. Mandelbrot, *A class of multifractal measures with negative (latent) values for the 'dimension' $f(\alpha)$* in Fractals' Physical Origin and Properties (Erice, 1988). L. Pietronero, ed., Plenum, 3–29.

[14] B. Mandelbrot, *Limit lognormal multifractal measures,* in Frontiers of Physics: Landau Memorial Conference (1988) E. A. Gotsman et al, eds. Pergamon, 309–340.

[15] B. Mandelbrot, *Two meanings of multifractality, and the notion of negative fractal dimension,* in Chaos: Soviet-American Perspectives on Nonlinear Science, (1990) D. Campbell, ed., American Institute of Physics, 79–90.

[16] B. Mandelbrot, *Random multifractals: negative dimensions and the resulting limitations of the thermodynamic formalism,* Proc. Royal Soc. (London) **A434** (1991), 79-88.

[17] B. Mandelbrot, *Negative dimensions and Hölders, multifractals and their Hölder spectra, and the role of lateral preasymptotics in science,* J. Fourier Analysis and its Applications, Special J. P.Kahane issue (1995), 409–432.

[18] B. Mandelbrot, *Multifractal power-law distributions, other 'anomalies,' and critical dimensions, explained by a simple example,* J. Stat. Phys. **110** (2003), 739–777.

[19] B. Mandelbrot, M. Frame, *A primer of multifractal measures, of negative test dimensions due to randomness, and of supersampling to move them from latent to manifest,.*